Ce-doped and Ce/Au-codoped alumino-phospho-silicate fibers: Spectral attenuation trends at high-energy electron irradiation and posterior low-power optical bleaching

A.V. Kir'yanov,[1,4*] S. Ghosh, M.C. Paul,[2] Y.O. Barmenkov,[1] V. Aboites,[1] and N. S. Kozlova[3]

[1]*Centro de Investigaciones en Optica, Loma del Bosque 115, Col. Lomas del Campestre, Leon 37150, Mexico*
[2]*Fiber Optics and Photonic Division, Central Glass & Ceramic Research Institute-CSIR, 196, Raja S.C. Mullick Road, Kolkata-700 032, India*
[3]*National University of Science and Technology (MISIS), Leninsky Avenue 4, Moscow 119049, Russia*
[4]*M.V. Lomonosov Moscow State University, Physics Department, Vorob'evy Gory, Moscow 119991, Russia*
[*]*kiryanov@cio.mx*

Abstract: We report a study of attenuation spectra' transformations in a couple of Cerium (Ce) doped alumino-phospho-silicate fibers (one of them codoped with gold (Au)), occurring under irradiation by a beam of high-energy β-electrons. The experimental data reveals an essential effect of β-irradiation upon the absorptive properties of the fibers, given by noticeable susceptibility of Ce ions in Ce^{3+}/Ce^{4+} valence states to the treatment, arisen as growth followed by saturation of induced absorption. We also report posterior bleaching of the β-darkened fibers, also in terms of attenuation spectra' transformations, at exposing them to low-power green (a He-Ne laser) and UV (mercury lamp) light, the effect never reported for Ce-doped fibers. It is shown that both phenomena are less expressed in Ce fiber codoped with Au than in Au-free one and that the spectral changes in the former are more regular and plain *vs.* irradiation dose and bleaching time. Possible mechanisms responsible for the phenomena and their impact at using such fibers for dosimetry and other applications are discussed.

OCIS codes: (160.5690) Rare-earth-doped materials; (060.2290) Fiber materials; (160.2750) Glass and other amorphous materials; (300.6250) Spectroscopy, condensed matter; (350.5610) Radiation.

References and links

1. J. W. Berthold III, "Overview of prototype fiber optic sensors for future application in nuclear environments," Proc. SPIE **2425**, 74–83 (1994).
2. F. Berghmans, O. Deparis, S. Coenen, M. Decréton, and P. Jucker, "Optical fibres in nuclear radiation environments: potential applications radiation effects need for standards," in *Trends in Optical Fibre Metrology and Standards*, O.D.D. Soares, ed. (NATO ASI Series E: Applied Sciences, Kluwer Academic, 1995), vol. 285, pp. 131–156.
3. J. K. Partin, "Radiation response of optical fibers in a nuclear reactor," Proc. SPIE **506**, 42–49 (1984).
4. P. Liu, X. Bao, K. Brown, and N. Kulkarni, "Gamma-induced attenuation in normal single- and multi-mode, Ge-doped and P-doped optical fibers: A fiber optic dosimeter for low dose levels," Can. J. Phys. **78**(2), 89–97 (2000).
5. M. C. Paul, D. Bohra, A. Dhar, R. Sen, P. K. Bhatnagar, and K. Dasgupta, "Radiation response behavior of high phosphorous doped step-index multimode optical fibers under low dose gamma irradiation," J. Non-Crystal. Sol. **355**, 1496–1507 (2009).
6. S. Ghosh, S. Das, M. C. Paul, K. Dasgupta, D. Bohra, H. S. Chaudhary, L. Panwar, P. K. Bhatnagar, and S. G. Vaijapurkar, "Evaluation of the performance of high phosphorous with germanium codoped multimode optical fiber for use as a radiation sensor at low dose rates," Appl. Opt. **50**(25), E80–E85 (2011).
7. S. C. Jones, J. A. Sweet, P. Braunlich, J. M. Hoffman, and J. E. Hegland, "A remote fibre optic laser TLD system," Rad. Prot. Dos. **47**, 525–528 (1993).
8. A. L. Houston, B. L. Justus, P. L. Falkenstein, R. W. Miller, H. Ning, and R. Altemus, "Remote optical fiber dosimetry," Nucl. Instrum. Methods Phys. Res. B **184**(1-2), 55–67 (2001).

#198435 - $15.00 USD Received 30 Sep 2013; revised 2 Dec 2013; accepted 3 Dec 2013; published 7 Feb 2014

9. C. Canevali, M. Mattoni, F. Morazzoni, R. Scotti, M. Casu, A. Musinu, R. Krsmanovic, S. Polizzi, A. Speghini, and M. Bettinelli, "Stability of luminescent trivalent Cerium in silica host glasses modified by Boron and Phosphorus," J. Am. Chem. Soc. **127**(42), 14681–14691 (2005).
10. M. Nikl, K. Nitsch, E. Mihokova, N. Solovieva, J. A. Mares, P. Fabeni, G. P. Pazzi, M. Martini, A. Vedda, and S. Baccaro, "Efficient radioluminescence of the Ce^{3+}-doped Na-Gd phosphate glasses," Appl. Phys. Lett. **77**(14), 2159–2161 (2000).
11. S. Baccaro, R. Dall'Igna, P. Fabeni, M. Martini, J. A. Mares, F. Meinardi, M. Nikl, K. Nitsch, G. P. Pazzi, P. Polato, C. Susini, A. Vedda, G. Zanella, and R. Zannoni, "Ce^{3+} or Tb^{3+} -doped phosphate and silicate scintillating glasses," J. Lumin. **87-89**, 673–675 (2000).
12. T. Murata, M. Sato, H. Yoshida, and K. Morinaga, "Compositional dependence of ultraviolet fluorescence intensity of Ce^{3+} in silicate, borate, and phosphate glasses," J. Non-Crystal. Sol. **351**, 312–316 (2005).
13. M. Laroche, S. Girard, R. Moncorge, M. Bettinelli, R. Abdulsabirov, and V. Semashko, "Beneficial effect of Lu^{3+} and Yb^{3+} ions in UV laser materials," Opt. Mater. **22**(2), 147–154 (2003).
14. Q. Fu, H. Saltsburg, and M. Flytzani-Stephanopoulos, "Active nonmetallic Au and Pt species on Ceria-based water-gas shift catalysts," Science **301**(5635), 935–938 (2003).
15. X. Wang, J. A. Rodriguez, J. C. Hanson, M. Pérez, and J. Evans, "In situ time-resolved characterization of Au-CeO_2 and AuO_x-CeO_2 catalysts during the water-gas shift reaction: Presence of Au and O vacancies in the active phase," J. Chem. Phys. **123**(22), 221101 (2005).
16. E. J. Friebele, "Radiation protection of fiber optics materials: Effect of cerium doping on the radiation-induced absorption," Appl. Phys. Lett. **27**(4), 210–212 (1975).
17. E. V. Anoikin, A. N. Guryanov, D. D. Gusovsky, E. M. Dianov, V. M. Mashinsky, S. I. Miroshnichenko, V. B. Neustruev, V. A. Tikhomirov, and Yu. B. Zverev, "UV and gamma radiation damage in silica glass and fibres doped with germanium and cerium," Nucl. Instrum. Methods Phys. Res. B **65**(1-4), 392–396 (1992).
18. A. Vedda, N. Chiodini, D. Di Martino, M. Fasoli, S. Keffer, A. Lauria, M. Martini, F. Moretti, G. Spinolo, M. Nikl, N. Solovieva, and G. Brambilla, "Ce^{3+}–doped optical fibres for remote radiation dosimetry," Appl. Phys. Lett. **85**(26), 6356–6358 (2004).
19. N. Chiodini, G. Brambilla, A. Vedda, D. Di Martino, M. Fasoli, A. Lauria, M. Redaelli, and E. Rosetta, "SiO_2 – based scincillating fibres for X-ray detection," Proc. SPIE **5198**, 298–305 (2004).
20. J. L. Cruz, F. Lliso-Valverde, M. V. Andres, and J. Perez-Calatayud, "Induced attenuation in Ce and Nd doped fibers irradiated with electron beams under low dose regime," Opt. Commun. **252**(4-6), 286–291 (2005).
21. E. Mones, I. Veronese, F. Moretti, M. Fasoli, G. Loi, E. Negri, M. Brambilla, N. Chiodini, and A. Vedda, "Feasibilty study for the use of Ce^{3+}–doped optical fibers in radiotherapy," Nucl. Instrum. Methods Phys. Res. A **562**(1), 449–455 (2006).
22. E. Mones, I. Veronese, A. Vedda, G. Loi, M. Fazoli, F. Moretti, N. Chiodini, B. Canillo, and M. Brambilla, "Ce-doped optical fibre as radioluminescent dosimeter in radiotherapy," Rad. Measur. **43**(2-6), 888–892 (2008).
23. M. M. Broer, R. L. Cone, and J. R. Simpson, "Ultraviolet-induced distributed-feedback gratings in Ce^{3+} -doped silica optical fibers," Opt. Lett. **16**(18), 1391–1393 (1991).
24. L. Dong, J. L. Archambault, L. Reekie, P. S. Russell, and D. N. Payne, "Bragg gratings in Ce^{3+}-doped fibers written by a single excimer pulse," Opt. Lett. **18**(11), 861–863 (1993).
25. H. Poignant, S. Boj, E. Delavaque, M. Monerie, T. Taunay, P. Niay, P. Bernaje, and W. X. Xie, "Ultraviolet-induced permanent Bragg gratings in Ce-doped fluorozirconate glasses or optical fibers," J. Non-Crystal. Sol. **184**, 282–285 (1995).
26. T. Taunay, P. Bernage, M. Douay, W. X. Xie, G. Martinelli, P. Niay, J. F. Bayon, E. Delavaque, and H. Poignant, "Ultraviolet-enhanced photosensitivity in cerium-doped aluminosilicate fibers and glasses through high-pressure hydrogen loading," J. Opt. Soc. Am. B **14**(4), 912–925 (1997).
27. M. Saad, L. R. Chen, and X. Gu, "Highly reflective fiber Bragg gratings inscribed in Ce/Tm co-doped ZBLAN fibers," IEEE Photon. Technol. Lett. **25**(11), 1066–1068 (2013).
28. Z. Meng, T. Yoshimura, K. Fukue, M. Higashihata, Y. Nakata, N. J. Vasa, and T. Okada, "Large improvement in quantum fluorescence yield of Er^{3+}–doped fluorezirconate and fluoroindate glasses by Ce^{3+} codoping," J. Appl. Phys. **88**(5), 2187–2190 (2000).
29. B.-M. Dicks, F. Heine, K. Petermann, and G. Huber, "Characterization of a radiation-hard single-mode Yb-doped fiber amplifier at 1064 nm," Laser Phys. **11**, 134–137 (2001).
30. S. S.-H. Yam, Y. Akasaka, Y. Kubota, R. Huang, D. L. Harris, and J. Pan, "Transient dynamics of fluoride-based high concentration Erbium–Cerium codoped fiber amplifier," IEEE Photon. Technol. Lett. **16**(2), 425–427 (2004).
31. M. Engholm, P. Jelger, F. Laurell, and L. Norin, "Improved photodarkening resistivity in ytterbium-doped fiber lasers by cerium codoping," Opt. Lett. **34**(8), 1285–1287 (2009).
32. P. Jelger, M. Engholm, L. Norin, and F. Laurell, "Degradation-resistant lasing at 980 nm in a Yb/Ce/Al-doped silica fiber," J. Opt. Soc. Am. B **27**(2), 338–342 (2010).
33. M. Vivona, S. Girard, C. Marcandella, T. Robin, B. Cadier, M. Cannas, A. Boukenter, and Y. Ouerdane, "Influence of Ce codoping and H pre-loading on Er/Yb-doped fiber: Radiation response characterized by Confocal Micro-Luminescence," J. Non-Crystal. Sol. **357**, 1963–1965 (2011).
34. M. Vivona, S. Girard, T. Robin, B. Cadier, L. Vaccaro, M. Cannas, A. Boukenter, and Y. Ouerdane, "Influence of Ce^{3+} codoping on the photoluminescence excitation channels of phosphosilicate Yb/Er-doped glasses," IEEE Photon. Technol. Lett. **24**(6), 509–511 (2012).
35. S. Girard, M. Vivona, A. Laurent, B. Cadier, C. Marcandella, T. Robin, E. Pinsard, A. Boukenter, and Y. Ouerdane, "Radiation hardening techniques for Er/Yb doped optical fibers and amplifiers for space application," Opt. Express **20**(8), 8457–8465 (2012).

#198435 - $15.00 USD Received 30 Sep 2013; revised 2 Dec 2013; accepted 3 Dec 2013; published 7 Feb 2014

36. A. Winterstein, S. Manning, H. Ebendorff-Heidepriem, and L. Wondraczek, "Luminescence from bismuth-germanate glasses and its manipulation through oxidants," Opt. Mater. Express **2**(10), 1320–1328 (2012).
37. S. Unger, A. Schwuchow, S. Jetschke, S. Grimm, A. Scheffel, and J. Kirchhof, "Optical properties of cerium-codoped high power laser fibers," Proc. SPIE **8621**, 862116 (2013).
38. A. V. Kir'yanov, V. V. Dvoyrin, V. M. Mashinsky, N. N. Il'ichev, N. S. Kozlova, and E. M. Dianov, "Influence of electron irradiation on optical properties of Bismuth doped silica fibers," Opt. Express **19**(7), 6599–6608 (2011).
39. K. Farah, A. Mejri, F. Hosni, A. H. Hamzaoui, and B. Boizot, "Formation and decay of colour centres in a silicate glasses exposed to gamma radiation: Application to high-dose dosimetry," in *Current Topics in Ionizing Radiation Research*, M. Nenoi, ed. (InTech, 2012).
40. J. S. Stroud, "Photoionization of Ce^{3+} in glass," J. Chem. Phys. **35**(3), 844–850 (1961).
41. J. S. Stroud, "Color centers in a cerium-containing silicate glass," J. Chem. Phys. **37**(4), 836–841 (1962).
42. J. S. Stroud, "Color-center kinetics in cerium-containing glass," J. Chem. Phys. **43**(7), 2442–2450 (1965).
43. G. Blasse and A. Bril, "Investigation of some Ce^{3+} activated phosphors," J. Chem. Phys. **47**(12), 5139–5145 (1967).
44. G. E. Malashkevich, E. N. Poddenezhny, I. M. Melnichenko, and A. A. Boiko, "Optical centers of cerium in silica glasses obtained by the sol-gel process," J. Non-Crystal. Sol. **188**, 107–117 (1995).
45. A. Patra, D. Kundu, and D. Ganguli, "Spectroscopic study of cerium-doped silica gel monoliths and their densified derivatives," J. Sol-Gel Sci. Technol. **9**(1), 65–69 (1997).
46. S. X. Lian, M. Ren, J. H. Lin, Z. N. Gu, and M. Z. Su, "On the afterglow of the cerium doped silicate glasses," J. Mater. Sci. Lett. **19**(18), 1603–1605 (2000).
47. G. Q. Xu, Z. X. Zheng, W. M. Tang, and Y. C. Wu, "Spectroscopic properties of Ce^{3+} doped silica annealed at different temperatures," J. Lumin. **124**(1), 151–156 (2007).
48. J. Bei, G. Qian, X. Liang, S. Yuan, Y. Yang, and G. Chen, "Optical properties of Ce^{3+}-doped oxide glasses and correlations with optical basicity," Mater. Res. Bull. **42**(7), 1195–1200 (2007).
49. S. Y. Marzouk and F. M. Ezz-Eldin, "Optical study of Ce^{3+} ion in gamma-irradiated binary barium-borate glasses," Phys. B **403**(18), 3307–3315 (2008).
50. R.-X. Xing, Y.-B. Sheng, Z.-J. Liu, H.-Q. Li, Z.-W. Jiang, J.-G. Peng, L.-Y. Yang, J.-Y. Li, and N.-L. Dai, "Investigation on radiation resistance of Er/Ce co-doped silicate glasses under 5 kGy gamma-ray irradiation," Opt. Mater. Express **2**(10), 1329–1335 (2012).
51. A. Bahadur, Y. Dwivedi, and S. B. Rai, "Optical properties of cerium doped oxyfluoroborate glass," Spectrochim. Acta A Mol. Biomol. Spectrosc. **110**, 400–403 (2013).
52. C. Jiang, Q. Zeng, and F. Gan, "New scincillator: Cerium-doped oxide glass," Proc. SPIE **4134**, 329–335 (2000).
53. E. E. Trusova, N. M. Bobkova, V. S. Gurin, and E. A. Tyavlovskaya, "Nature of color centers in silicate glasses with additions of cerium and titanium oxides," Glass and Ceram. **66**(7-8), 240–244 (2009).
54. W.-Y. Cong, S.-M. Li, Y.-J. Wang, L. Tao, X.-Y. Liu, and W.-M. Zheng, "Photoluminescence study of Ce-doped silica films," J. Lumin. **132**(1), 161–163 (2012).
55. G. P. Singh, P. Kaur, S. Kaur, R. Kaur, and D. P. Singh, "Conversion of Ce^{3+} to Ce^{4+} ions after gamma ray irradiation on CeO_2-PbO-B_2O_3 glasses," Phys. B **408**, 115–118 (2013).
56. D. L. Griscom, M. E. Gingerich, and E. J. Friebele, "Radiation-induced defects in glasses: Origin of power-law dependence of concentration on dose," Phys. Rev. Lett. **71**(7), 1019–1022 (1993).
57. V. A. Mashkov, W. R. Austin, L. Zhang, and R. G. Leisure, "Fundamental role of creation and activation in radiation-induced defect production in high-purity amorphous SiO_2," Phys. Rev. Lett. **76**(16), 2926–2929 (1996).
58. D. Griscom, "Fractal kinetics of radiation-induced point-defect formation and decay in amorphous insulators: Application to color centers in silica-based optical fibers," Phys. Rev. A **64**, 174201 (2001).
59. E. M. Dianov, L. S. Kornienko, E. P. Nikulin, A. O. Rybaltovskii, and P. V. Chernov, "Reversible optical bleaching of the induced absorption in fiber-optic waveguides," Sov. J. Quant. Electron. **9**(5), 636–637 (1979).
60. E. J. Friebele and M. E. Gingerich, "Photobleaching effects in optical fiber waveguides," Appl. Opt. **20**(19), 3448–3452 (1981).
61. E. M. Dianov, L. S. Kornienko, E. P. Nikulin, A. O. Rybaltovskii, and P. V. Chernov, "Influence of the temperature and optical power level on induced absorption in fiber-optic waveguides of pure quartz glass," Sov. J. Quant. Electron. **11**(9), 1171–1177 (1981).
62. Y. Zhu, S. Ouyang, S. Gao, and W. Teng, "Luminescence characteristics of Ce^{3+} doped Ca-Al-Ba glass," J. Wuhan Univ. Techn. **24**(5), 815–818 (2009).
63. D. Jia, "Relocalization of Ce^{3+} 5d electrons from host conduction band," J. Lumin. **117**(2), 170–178 (2006).
64. X. Yue, A. Adibi, T. Hudson, K. Buse, and D. Psaltis, "Role of cerium in lithium niobate for holographic recording," J. Appl. Phys. **87**(9), 4051–4055 (2000).
65. A. Lin and W.-T. Han, "Recent progress in development and nonlinear optical device application of optical fibers incorporated with noble metal nanoparticles," Proc. SPIE **7095**, 70950G (2008).
66. L. F. Koao, H. C. Swart, R. I. Obed, and F. B. Dejene, "Synthesis and characterization of Ce^{3+} doped silica (SiO_2) nanoparticles," J. Lumin. **131**(6), 1249–1254 (2011).

1. Introduction

Nowadays, development of suitable host glasses and fibers for dosimetry applications based on formation of radiation induced defects leading to glass coloration [1–6] or on filling of

#198435 - $15.00 USD Received 30 Sep 2013; revised 2 Dec 2013; accepted 3 Dec 2013; published 7 Feb 2014

pre-existing traps, measured by means of thermally or optically stimulated fluorescence [7], becomes a hot task. Such dosimetry systems can be used in high radiation fields, for example, in proximity to nuclear reactors, hazardous places, and in open space. They can be also applicable in the conditions of diagnostic or radiotherapy irradiations for a careful control of the dose imparted to patients. Optical fiber dosimeters are being intensively investigated and recently a few systems have been proposed and implemented based on versatile physical effects in radiation-sensitive silica fibers [8]. The advantages of a fiber based dosimeter is that its kernel, a specialty fiber, has structural and refractive index properties similar to the ones of pure SiO_2 glass and that it is compatible with commercial fibers, making its use invaluable in a remote place where direct access is denied.

In particular, Cerium (Ce) doped silica glass has interesting properties of fluorescence [9], which makes it a promising material to be used as a scintillator for detecting x- and γ-rays, or neutrons [10,11], as well as in tunable solid-state lasers operating in the near-UV, violet, and blue regions [12,13]. On the other hand, silica glass is known to suffer from the presence of point defects and OH groups, which are responsible for non-radiative recombination channels competing fluorescence. In turn, gold (Au) combined with cerium oxide CeO_2 was reported to be a promising catalyst for the reaction $CO + H_2O \rightarrow H_2 + CO_2$ [14,15], giving a possible way to remove carbon-related impurities along with OH groups from the silica matrix during synthesis. Thus, Ce/Au co-doped glass host is expected to enhance efficiency of energy transfer from the host glass matrix to the emissive centers. The other motivation for Au co-doping of Ce-doped glass (and fibers) is to increase its radiation resistance, which is argued in more details in the discussion section. Furthermore, Ce-doped glass with minor amount of phosphorous (P) inhibits both CeO_2 segregation and oxidation of isolated Ce^{3+} ions to Ce^{4+} ones [9]. Apparently, the refereed properties of alunimo-phospho-silicate glass doped with Ce and Ce/Au should also apply for optical fibers made on its base. In the meantime, the use of Ce doped silica fibers for dosimetry through a measurement of induced loss produced by different irradiation kinds is still a matter to study.

Our present research highlights novelties stemming from the experiments on irradiating Ce-doped alumino-phospho-silicate fibers by a beam of free electrons of high energy (further – β-irradiation), resulted in darkening of the fibers. We show that the irradiated fibers are sensitive to the action of weak optical radiation of a He-Ne laser (543 nm) and UV mercury lamp, both leading to partial recovery of their initial properties. The whole of experimental data evidences notable sensitivity of Ce-doped fibers to both kinds of treatment. Furthermore, it is found that the spectral transformations occurring in Ce fiber codoped with Au are less expressed but more regular and plain upon β-irradiation dose and upon exposure time at bleaching than in Au-free one. A brief discussion in attempt of a reasonable explanation of the experimental laws completes the study where the key point is a discussion about the species involved in the processes, which are associated with Ce doping.

The reported results may have value at using Ce-doped optical fibers for dosimetry in harmful environments [8,16–22] and for inscribing fiber Bragg gratings in such fibers [23–27]. Furthermore, given by renewed interest to Ce codoping as a method to diminish photodarkening in Yb doped fibers and for optimizing the performance of Er, Yb/Er, and Bismuth doped fibers in the presence of ionizing radiations and in space technologies [28–37], our present results seem to be also relevant.

2. Fibers fabrication and experimental techniques for their studying

2.1. Fibers' fabricating route

Ce-doped and Ce/Au-codoped fiber preforms based on alumino-phospho-silicate glass host have been made by means of the modified chemical vapour deposition (MCVD) process in-line with the solution doping (SD) technique. Fabricating of the preforms was made through deposition of five porous SiO_2-P_2O_5 layers at 1500 ± 10°C. After complete deposition of the porous un-sintered layers, the deposition tube was removed from the MCVD lathe and placed into the SD setup. Aqueous solutions of suitable strength of $AlCl_3$, $6H_2O$, $CeCl_3$, and $7H_2O$

#198435 - $15.00 USD Received 30 Sep 2013; revised 2 Dec 2013; accepted 3 Dec 2013; published 7 Feb 2014

and $AlCl_3$, $6H_2O$, CeC_3, $7H_2O$, and $AuCl_3$ were used for making, correspondingly, the Ce and Ce/Au preforms; in both cases, the solution soaking period was continued for 45 minutes. After completing the SD process, the deposition tube was mounted again into the MCVD lathe where dehydration and oxidation were gradually performed at temperatures around 900-1000°C. Sintering of the soaked porous layers was done slowly in the MCVD process, by increasing temperature from 1500 to 2000°C. After that, the tube was collapsed to convert into the optical preform. The final fibers have been drawn using a standard fiber drawing tower and on-line dual-resin coating. The parameters of the fabricated Ce-doped and Ce/Au-codoped fibers are given in Table 1.

Table 1. Basic properties of Ce-doped and Ce/Au-codoped fibers

Fiber #	*Core Composition*	*Core Diameter (μm)*	*Core NA*
"Ce"	$SiO_2 + P_2O_5 + CeO_2 + Al_2O_3$	25	0.15
"Ce/Au"	$SiO_2 + P_2O_5 + CeO_2 + Al_2O_3 + Au_2O_3$	25	0.16

Estimated from EDX, average doping levels were found to be 5.0 wt.% Al_2O_3, 0.15 wt.% P_2O_5, 0.3 wt.% CeO_2 (in Ce-doped fiber) and 5.1 wt.% Al_2O_3, 0.15 wt.% P_2O_5, 0.27 wt.% CeO_2, and 0.2 wt.% Au_2O_3 (in Ce/Au-codoped fiber). Both fibers presented multimode waveguide properties, given by their large cores which make them useful for sensor applications. A sample of standard multimode Al-doped (~6 wt.% Al_2O_3) fiber was used in experiments for comparison.

2.2. Experimental techniques

A controllable linear accelerator of the LU type which emits β-electrons with a narrow-band energy spectrum (~6 MeV) in a short-pulse (~5-μs) mode was used for irradiating the fibers [38]. Fiber samples with lengths measured of around 2 m were irradiated when placed into the accelerator's chamber for various time intervals, which provided growing irradiation doses. The β-irradiation dosage on some of the figures below corresponds to 1×10^{12} (dose 1), 5×10^{12} (dose 2), 1×10^{13} (dose 3), 5×10^{13} (dose 4), 1×10^{14} (dose 5), and 2.5×10^{15} (dose 6) cm^{-2}. The irradiated fibers were leaved for 2 weeks prior to the main-course spectral measurements to avoid the role of short-living components in decay of induced absorption (IA) [39]. The measurements were done during limited time (during the following 2 weeks) for diminishing the role of spontaneous IA recovering. Note that ionization, *i.e.* the production of β-induced carriers by an electron beam (i.e. of secondary free holes and electrons) is the main cause of the spectral transformations in the fibers. This happens because high-energy primary β-electrons are virtually non-dissipating at the propagation through the fiber samples (125 μm in diameter); on the other hand, certain contribution in ionization of the fibers' glass arises from γ-quanta born at inelastic scattering of the high-energy electrons.

The optical transmission spectra of fiber samples were measured (employing the cutback method), using a white-light source with fiberized output and an optical spectrum analyzer (OSA) with 5-nm resolution. The spectra were recorded before and after each stage of β-irradiation (doses 1 to 6, see above) and during posterior exposure to a He-Ne laser (543 nm) or UV lamp ($\lambda < 450$ nm). The length of the fiber samples was varied from a few to tens centimeters (β-darkened and optically bleached fibers) to tenths of meters (pristine fibers) to ensure accuracy of measurements. The attenuation spectra presented below were obtained after recalculating the measured transmissions into the losses [dB/m]. In some of the figures the difference spectra in terms of IA are given, which were obtained after subtraction of the attenuation spectra of pristine samples from the ones recorded after a certain dose of β-irradiation; this allows a straightforward view on the net spectral loss changes in the darkened fibers.

The transmission dynamics at optical bleaching of β-darkened fibers by 543-nm light was inspected applying frontal detecting geometry where a beam of a He-Ne laser was coupled through a micro-objective into the fiber sample (~1…2 cm in length) and transmitted light

#198435 - $15.00 USD Received 30 Sep 2013; revised 2 Dec 2013; accepted 3 Dec 2013; published 7 Feb 2014

was detected using a Si photo-detector connected to a multi-meter. This permitted detection of the changes in the samples' transmission *in situ*. The results of these measurements are given below in terms of absorption difference (AD) at bleaching with respect to the initial (β-darkened) state of the samples. At the last, in the experiments on optical bleaching of β-irradiated fibers using UV light we measured, also *in situ*, transmission change of the samples at long-term (tens of hours) exposure to low-density UV light; in this case ~12-cm pieces of fibers were used.

All experiments were made at room temperature.

3. Experimental results

3.1. Induced absorption as a result of β-irradiation

In this section the basic results of β-irradiation of the fibers are reported.

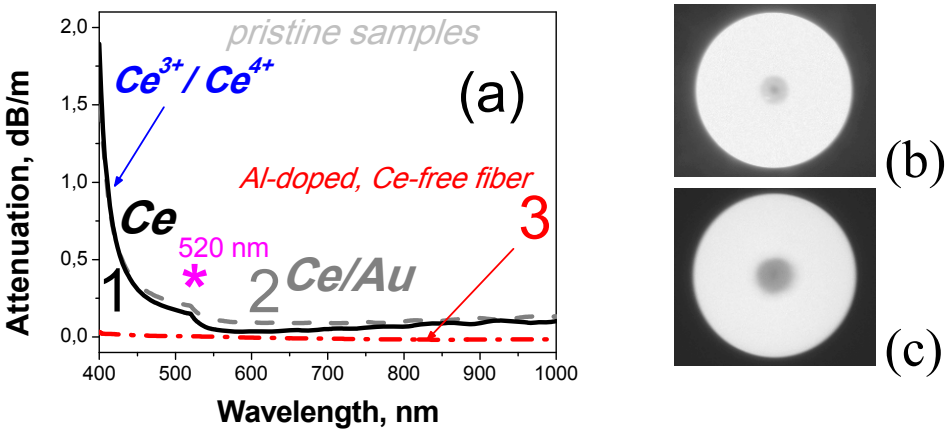

Fig. 1. (a) Attenuation spectra of pristine Ce-doped (curve 1), Ce/Au-codoped (curve 2), and Al-doped Ce-free (curve 3) fibers in a VIS-to-near-IR spectral range and micro-photographs of pristine Ce-doped (b) and Ce/Au-codoped (b) fibers.

In Fig. 1, we demonstrate (a) attenuation spectra of Ce-doped (black solid curve 1) and Ce/Au-codoped (grey dashed curve 2) fibers before irradiation, i.e. in "pristine" (as-received) state, and (b and c) the fibers' cross-section images, obtained using a microscopy tool of the Vytran equipment under white-light illumination. Rather long (meters) fiber lengths were used in the spectral measurements applying the cutback method whereas short (tens centimeters) pieces of fibers were used at microscopy. For comparison, spectral loss in the standard Al-doped Ce-free fiber is also shown in Fig. 1(a); see red dash-dotted curve 3.

We reveal from figure (a) that in the Ce-doped and Ce/Au-codoped fibers dramatic growth of absorption occurs towards UV, below ~550 nm, which is known to be a shoulder of the strong absorption bands of Ce^{3+}/Ce^{4+} ions (mostly pronounced in UV within a 200–350 nm spectral region; see e.g [25,26,31,34,40–51].). Apparently, there is no such feature in the Ce-free reference fiber. The other points to be noticed are steep loss rise in Ce-doped and Ce/Au-codoped fibers towards IR and a small peak at ~520 nm (shown by asterisk), the features not observed for the Ce-free fiber.

Figure 2 allows one to reveal the trends occurring in the fibers' attenuation spectra as the result of β-irradiation with moderate dose 4, equal to 1×10^{12} cm^{-2}. The equipment used to get these spectra was the same as in the experiments reported above. Only notice that in the last case the measurements were proceed with much shorter fiber samples (~a few cm) in virtue of strong IA established after β-irradiation.

It is seen that IA in the Ce-free fiber is in average ~2 times higher than in the Ce-doped and Ce/Au-codoped ones. The other fact deserving attention is that maxima of IA are

#198435 - $15.00 USD Received 30 Sep 2013; revised 2 Dec 2013; accepted 3 Dec 2013; published 7 Feb 2014

spectrally located nearby 400 and 500 nm in these fibers whereas the ones in the Ce-free fiber are at ~400 and ~600 nm, which allows their attribution to the well-known NBOHC's of two types; see e.g. [39].). However, since for the Ce-free fiber IA spectrum is not well "structured", the presence of other defect states, rather than NBOHC's (such as Si- and Al-related defect centers, the spectral contributions of which are masked by very extensive bands centered at ~400 and ~600 nm) cannot be excluded. Furthermore, one can see from photos (b) and (c) that in Ce-doped and Ce/Au-codoped fibers the core and adjacent core-cladding regions suffer from darkening after β-irradiation, in the former the effect being more pronounced than in the remainder of the fibers' clad areas.

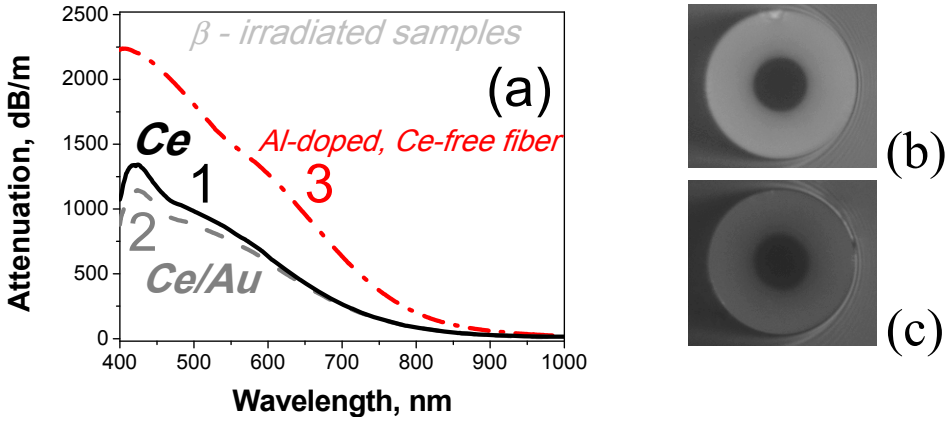

Fig. 2. (a) Attenuation spectra of Ce-doped (curve 1), Ce/Au-codoped (curve 2), and Al-doped Cerium-free (curve 3) fibers, all measured after β-irradiation with dose 4 (5×10^{13} cm^{-2}) and micro-photographs of Ce-doped (b) and Ce/Au-codoped (c) fibers recorded after irradiation with dose 4.

From Fig. 3, it is seen that IA in Ce-doped (a) and Ce/Au-codoped (b) fibers increases monotonously with increasing irradiation dose; this trend is mostly expressed over the wavelengths range 400–700 nm while for the rest of wavelengths it steadily vanishes. The other detail seen from Fig. 3 is that, for moderate doses (1 to 4), IA is higher for Ce-doped fiber than for Ce/Au-codoped one.

The two-maxima structure of the IA spectra becomes apparent at high irradiation doses for both (Ce-doped and Ce/Au-codoped) fibers, with the first maximum (higher in magnitude) being spectrally located at ~415 ± 10 nm and the second (less pronounced) – at ~520 ± 10 nm (compare with the small peak at ~520 nm asterisked in the attenuation spectra of pristine fibers; Fig. 1(a)).

To evaluate IA strength in the fibers as a function of β-irradiation dose, let's compare the IA spectra with the attenuation spectra of the same fibers being in pristine state; see Fig. 1. It is known [46–57] that strong growth of attenuation towards UV is common for Ce doped glasses, stemming from the transitions inherent to Ce^{3+}/Ce^{4+} ions. This is justified when comparing attenuations of the pristine Ce-doped and Ce/Au-codoped fibers with attenuation of pristine Ce free one; see above. [Unfortunately, IA arising in the UV-region, below 400 nm, could not be detected using our experimental equipment.] Regarding IA in the near-IR region, notice that the spectral transformations are more complicate here; see insets to Fig. 3. For instance, for both fibers a low-dose range where IA is negative exists. This can happen because slightly increasing attenuation towards near-IR in pristine Ce-doped and Ce/Au-codoped fibers (refer to Fig. 1) gets mitigated at β-irradiation due to some unclear at the moment mechanism. Probably a similar effect allowed authors of Ref [20]. to perform a sensing unit based on a Ce-doped silica fiber.

#198435 - $15.00 USD Received 30 Sep 2013; revised 2 Dec 2013; accepted 3 Dec 2013; published 7 Feb 2014

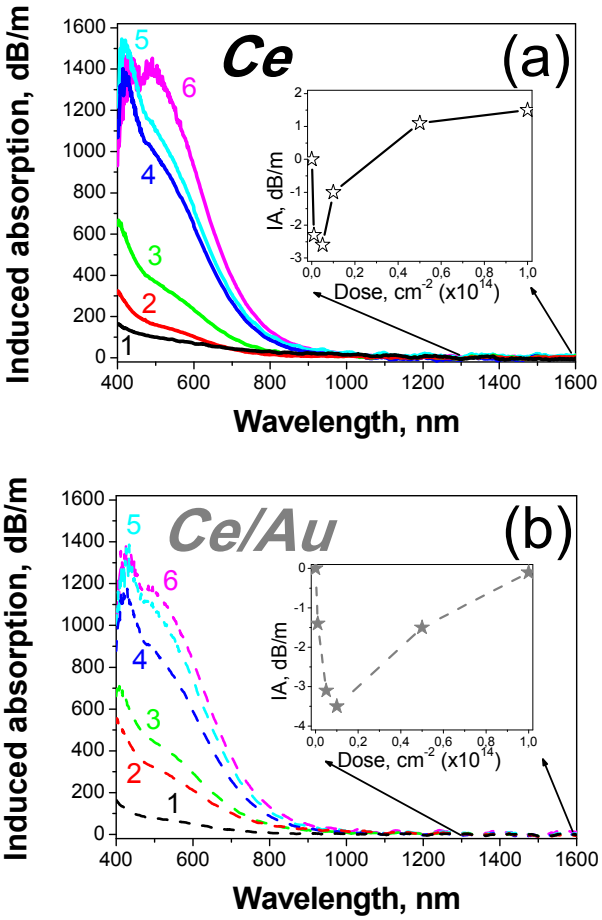

Fig. 3. Main frames: IA spectra of Ce-doped (a) and Ce/Au-codoped (b) fibers; curves 1 to 6 correspond to the following doses of irradiation (in both figures): 1×10^{12} (dose 1), 5×10^{12} (dose 2), 1×10^{13} (dose 3), 5×10^{13} (dose 4), 1×10^{14} (dose 5), and 2.5×10^{15} (dose 6) cm^{-2}. Insets: average attenuations within a 1300–1550-nm range *vs*. irradiation dose.

By making de-convolution of IA spectra (Fig. 3) within the 400–1000-nm spectral range, we demonstrate their two-band structure; the examples are demonstrated in insets to Fig. 4.

Spectral locations of the two bands (1 and 2) were found to be almost independent of β-irradiation dose for both fibers. These bands are centered at ~3.0 and ~2.4 (± 0.1) eV with half-widths at a 3-dB level being ~0.3 and ~0.5 (± 0.05) eV, correspondingly. When IA, represented by magnitudes of these two peaks, is plotted *vs.* irradiation dose, the dependences shown by blue (for band 1) and red (for band 2) symbols are obtained; see main frames of Figs. 4(a) and 4(b). Fitting of the dependences within a moderate range of doses (up to ~2×10^{13} cm^{-2}; see vertical black dotted lines in the figure) demonstrates a linear growth kinetics of IA in both bands *vs.* dose (at log-log scale); see the blue and red lines in the figure.

#198435 - $15.00 USD Received 30 Sep 2013; revised 2 Dec 2013; accepted 3 Dec 2013; published 7 Feb 2014

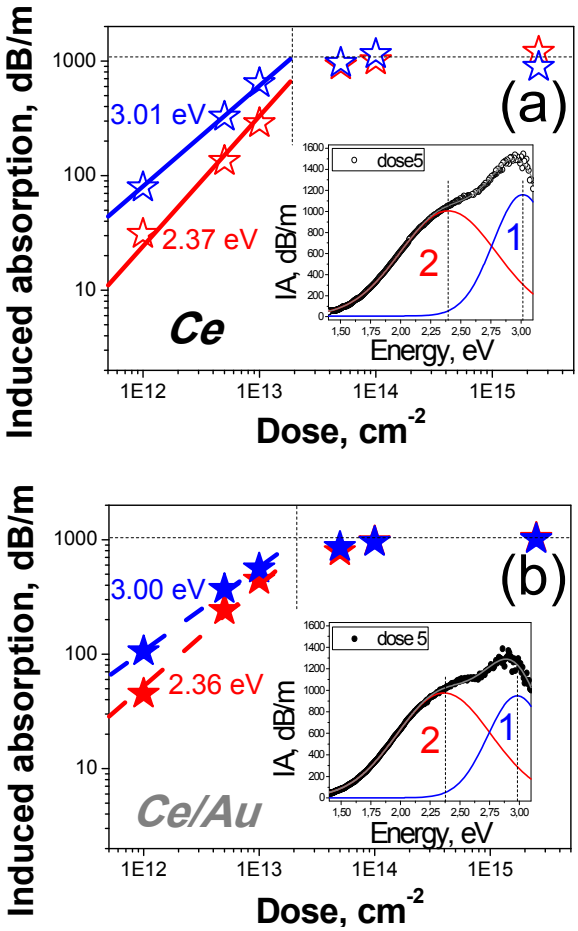

Fig. 4. Main frames: dose dependences of IA, measured for Ce-doped (a) and Ce/Au-codoped (b) fibers; blue and red symbols and lines show IA magnitudes of bands 1 and 2, obtained after deconvolution of the spectra shown in Fig. 3. Insets: examples of deconvolution of the data obtained for the fibers, irradiated with dose 5 (spectra are plotted in eV-domain).

The slopes' values estimated from fitting are measured by powers' values of ~1.7 (~1.2 dB/m/cm^2) (Ce-doped fiber) and ~1.3 (~0.9 dB/m/cm^2) (Ce/Au-codoped fiber), for bands 2 and 1, correspondingly. Interestingly, these ratios, on one hand, are almost equal for each fiber (~1.5) and, on the other hand, the slopes' ratios, when compared for bands 1 and 2, are also almost equal for Ce-doped and Ce/Au-codoped fibers (~1.3). At higher irradiation doses the experimental IA values, in both bands and for either fiber, steadily approach some "plateaus", marked by horizontal black dotted lines in the figures. Note that similar trends were discussed in the older literature; see e.g. the milestone works [56–58]. It is also interesting that IA in maxima of both bands 1 and 2 at the plateaus (for doses >2 × 10^{14} cm^{-2}) have virtually the same magnitudes (for both fibers).

3.2. Bleaching of induced absorption as a result of posterior exposure to 543-nm / UV light

Hereafter, the featuring results on optical bleaching of β-irradiated Ce-doped and Ce/Au-codoped fibers using a low-power He-Ne 543-nm laser and standard UV mercury lamp, having a spectral band limited from above by ~450 nm, are reported.

Keeping in mind that IA, originated from generation of color centers or defects in a glass matrix by different kinds of irradiation, can be "bleached" by light (which is known for long

#198435 - $15.00 USD Received 30 Sep 2013; revised 2 Dec 2013; accepted 3 Dec 2013; published 7 Feb 2014

time – see e.g. the first works [59–61]), we found interesting to check whether such treatment has effect in our case.

First, we inspected effect of weak 543-nm radiation delivered from a 1.5-mW He-Ne laser. In the experiments, power launched into both fibers was fixed at ~0.5 mW (overall coupling efficiency ~30%). We used in this case very short (1…2 cm) pieces of β-irradiated fibers, remembering about big IA measured by hundreds of dB/m (see Figs. 3 and 4).

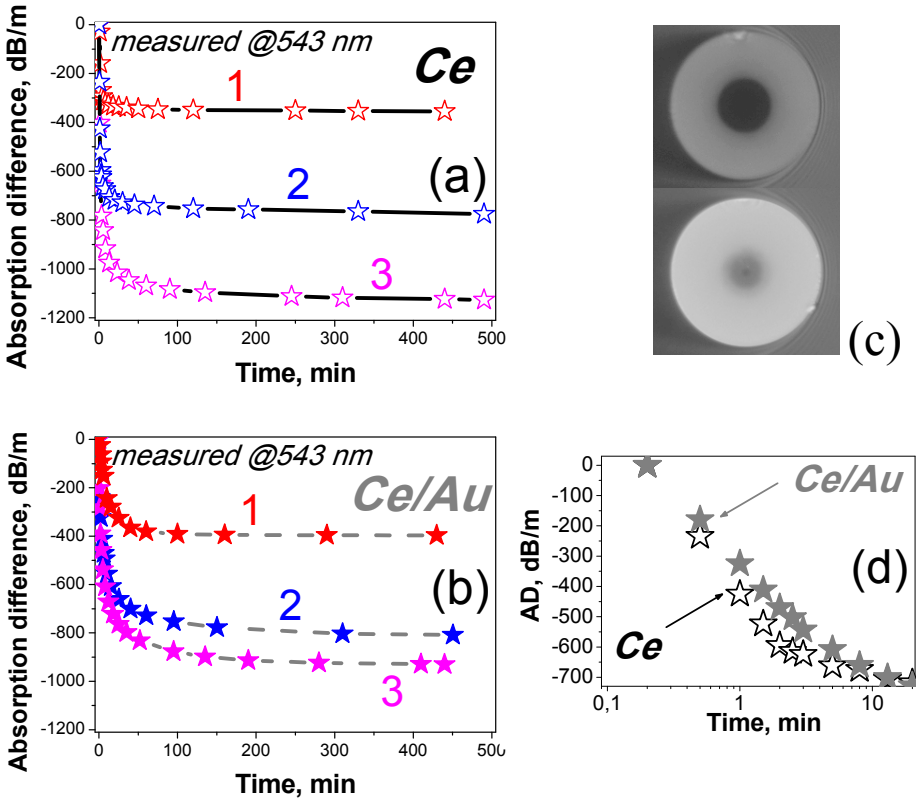

Fig. 5. Dynamics of attenuation decay in terms of AD in Ce-doped (a) and Ce/Au-codoped (b) fibers under the action of 543-nm light (~0.5-mW); bleaching (resulted in negative AD) was realized after β-irradiation with doses 2 (red curves 1), 4 (blue curves 2), and 6 (magenta curves 3), for which AD is taken to be zero. (c) Micro-photographs of darkened (dose 5 of β-irradiation) Ce-doped fiber prior to optical bleaching (top) and after bleaching during 7.5 hours (bottom). (d) Examples of the initial 543-nm bleaching stage, which zoom the dependences shown by curves 2 in figures (a) and (b), respectively.

Figure 5 presents the temporal dynamics of changes in attenuation of Ce-doped (a) and Ce/Au-codoped (b) fibers under the action of 543-nm light, measured at the same wavelength. The effect of partial bleaching of β-induced attenuation is apparent, that is, the negative values of AD. This means a partial recombination of defect centers, responsible for IA in both bands centered at ~3.0 and ~2.4 eV; refer to Fig. 4.

One may speculate that the bleaching effect observed in the Ce-doped and Ce/Au-codoped fibers is solely due to radiation induced recombination or, possibly due to thermal-induced recombination. As for us, the former appears to play a vital role in IA fading.

The bleaching effect is clearly demonstrated by the micro-photographs in Fig. 5(c), on the example of Ce-doped fiber. It is seen that the initial state (before β-irradiation) was practically restored in the fiber under the action of 543-nm light: Compare these photos with the one of pristine Ce-doped fiber shown in Fig. 1(b). Notice that optical bleaching of both fibers demonstrates a saturating decay kinetics and that the decay rate is higher in the fiber codoped

#198435 - $15.00 USD Received 30 Sep 2013; revised 2 Dec 2013; accepted 3 Dec 2013; published 7 Feb 2014

with Au than in the Au-free one (compare curves 1–3 in (a) and (b)); also notice an almost exponential character of bleaching at the start of the process (see Fig. 5(d)).

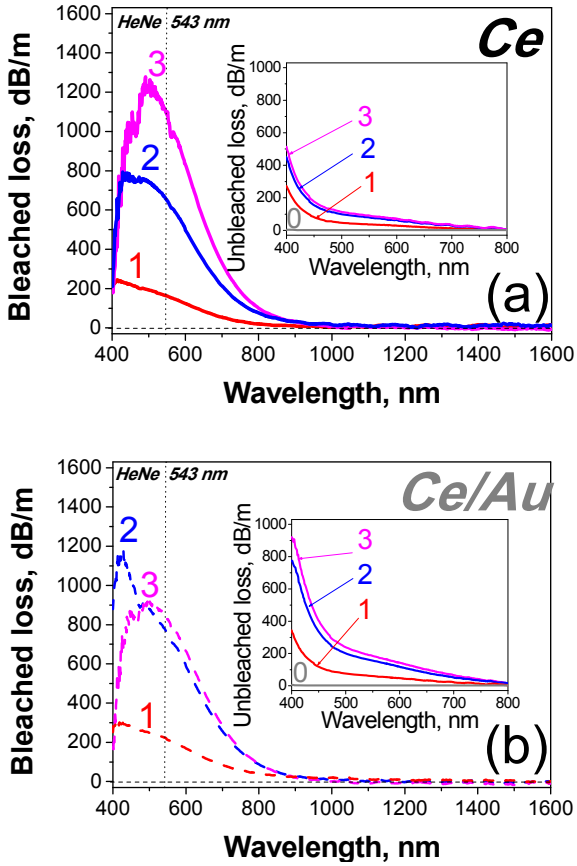

Fig. 6. Bleached (main frames) and unbleached (insets) spectral loss in Ce-doped (a) and Ce/Au-codoped (b) fibers after ~0.5-mW 543-nm treatment, posterior to β-irradiation with doses 2 (red curves 1), 4 (blue curves 2), and 6 (magenta curves 3). For comparison, curves 0 in the figures demonstrate the attenuation spectra of pristine fibers.

Figures 6(a) and 6(b) show how the bleached (main frames) and un-bleached (insets) loss in Ce-doped and Ce/Au-codoped fibers behave via 543-nm bleaching. Relaxation of IA is seen to be quite effective at exposure the fibers to 543-nm light, which appears to be attractive for applications. It also deserves mentioning that unbleached (or remnant) loss is higher in Ce/Au-codoped than in Ce-doped fiber, i.e. co-doping of a Ce-doped fiber with Au results in a similar effect of less sensitivity to exterior influence (compare with the results on β-irradiation). However, in the case of bleaching this appears to be a disadvantage.

The results on illuminating the darkened Ce-doped and Ce/Au-codoped fibers with UV light are shown in Fig. 7. In Fig. 7(a) we exemplify the dynamics of transmission of β-irradiated (dose 5) Ce/Au-codoped sample within a 400–1600 nm range. The micro-photographs in Fig. 7(b) visualize the result of treatment, being almost full fading of IA loss. This effect can be quantified by a shift of a wavelength's transmission, measured at a 3-dB level (see grey line in figure (a)), from near-IR to VIS. It is seen from Fig. 7(c), where we demonstrate the results of experiments with Ce/Au-codoped (black open dots) and Ce-doped (grey open squares) fibers, that it has a very similar trend in both fibers.

#198435 - $15.00 USD Received 30 Sep 2013; revised 2 Dec 2013; accepted 3 Dec 2013; published 7 Feb 2014

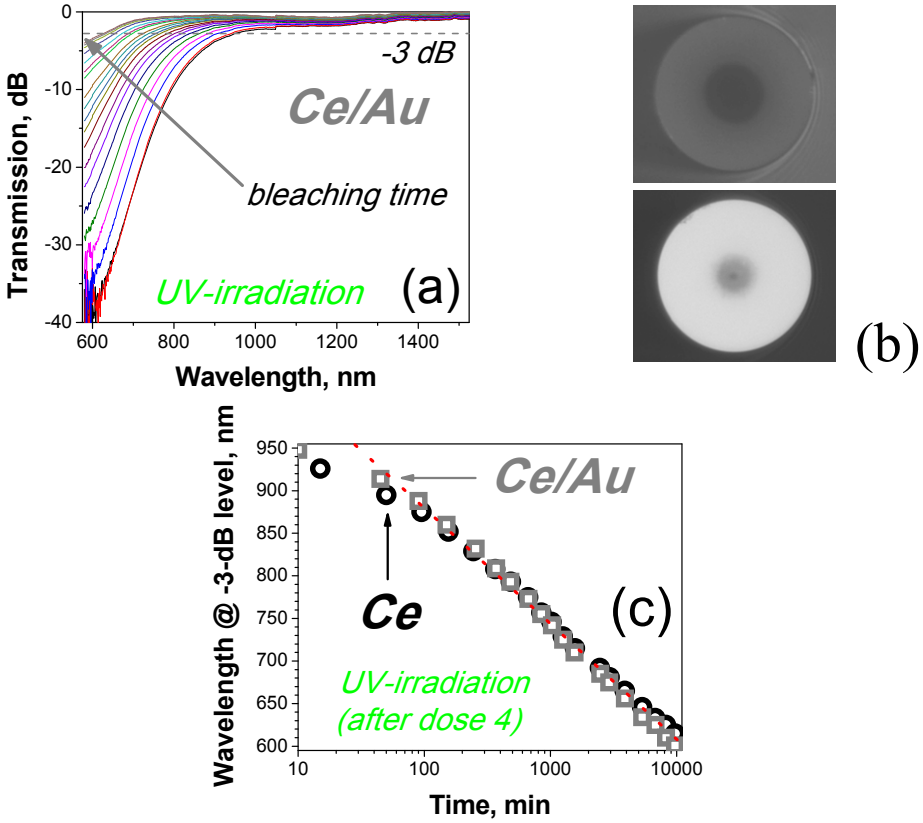

Fig. 7. (a) Dynamics of attenuation decay (in terms of transmission of Ce/Au-codoped fiber under UV-lamp illumination with maximal spectral power @350 nm). Bleaching was realized in the darkened fiber, posterior to β-irradiation with dose 4. (b) Micro-photographs of darkened (dose 5 of β-irradiation) Ce/Au-codoped prior to optical bleaching with UV-lamp (top) and after continuous bleaching during 10000 hours (bottom). (c) Examples of the spectral transformations during UV-bleaching in terms of shifting of the fiber's transmission edge wavelength measured at −3-dB level; the data were obtained for Ce/Au-codoped (open black dots) and Ce-doped (open grey squares) fibers, preliminary β-irradiated with dose 4; both the data are fitted to the eye by dotted red lines.

4. Discussion

4.1. Pristine fibers

Regarding the matter of pristine Ce-doped and Ce/Au-codoped fibers (see Fig. 1), apart from strong growth of absorption at shorter (VIS to UV) wavelengths, apparently connected with the presence of Ce in valence states Ce^{3+}/Ce^{4+} [25,26,31,34,40–51], the other two points deserve mentioning, namely, (*i*) monotonous growth of loss towards IR for both fibers (of not clear origin but apparently inherent to Ce doping since such a trend is absent in the Ce free reference fiber) and (*ii*) a distinct peak at ~520 nm (~2.4 eV), seen in the absorption spectra of both fibers (but also absent in the Ce free one). We suppose that this peak has the same origin as band 2 risen at β-irradiation and spectrally located as well at ~2.4 eV; see Fig. 4. This feature has not been reported for bulk Ce doped silica but is frequently observed in Ce doped fibers as the result of ionizing radiations [19,26,44,45]. It can be related [40–42] to quite stable $Ce^{3+}h^{+}$ centers, or alternatively while hypothetically, to $Ce^{4+}e^{-}$ centers (existence of which has not been documented so far), but apparently not to sole Ce ions either in trivalent or tetravalent state. There can be a reference to the "empirical" laws in attempt to relate such

#198435 - $15.00 USD Received 30 Sep 2013; revised 2 Dec 2013; accepted 3 Dec 2013; published 7 Feb 2014

centers to high overall Ce concentrations (>0.1 mol.%), glass basicity, oxidized fabrication ambience, or ionizing radiations of various kinds [19,41,46,48–53,55,62,63], leading to a shift of a Ce doped material's absorption edge towards longer wavelengths. All these circumstances are met, in a more or less degree, in our case. However as for us a more realistic cause for the existence of $Ce^{3+}h^{+}$ or/and $Ce^{4+}e^{-}$ defect centers in pristine fibers, attributable by the 520-nm peak, can be ionization, i.e. generation of free electrons e^{-} and holes h^{+}, at the fiber preform collapse stage [26] or at fiber drawing with posterior covering by acrylic outer cladding when – in both circumstances – strong UV light is produced, with a result being trapping of the free carriers by Ce^{3+}/Ce^{4+} species. However, the proposed idea needs a deeper exploration in future.

4.2. β-irradiated fibers

Consider, now in more details, the results of β-irradiation of Ce-doped and Ce/Au-codoped fibers (see Figs. 2–4). Let's propose that a common set of processes involved at irradiating the fibers with β-electrons (and resulted in IA rise followed by saturation and described by the "stretched-exponent" law [16,26,39,56–58]) comprises: (*i*) creating of secondary carriers (holes h^{+} and electrons e^{-}) in the core-glass matrix by energetic β-electrons and their trapping nearby imperfections of the glass such as Ce ions (Ce^{3+}/Ce^{4+}), non-bridging oxygen centers, other centers associated with Al and P, and oxygen vacancies; (*ii*) direct $h^{+} - e^{-}$ recombination (annihilation); (*iii*) thermally- or/and radiatively activated recombination between the centers or defects, generated during and after β-irradiation. Concerning the role of Ce-doping (our case), IA is assumed to be produced via irradiation-induced reactions $Ce^{3+} + h^{+} \rightarrow Ce^{3+}h^{+}(\rightarrow ?Ce^{4+})$ and $Ce^{4+} + e^{-} \rightarrow (?Ce^{4+}e^{-}) \rightarrow Ce^{3+}$ [26,31,33,40–42,50,55,63], implying Ce ions being in valences Ce^{3+}/Ce^{4+} are present in pristine samples or/and being generated through irradiation. Our motivations to think by this way are as follows. Notice that determination of relative contents of Ce^{3+}/Ce^{4+} ions in pristine silica glass or fiber is itself a complicate task and that at low Ce doping mainly fluorescing Ce^{3+} are formed in the glass while at higher overall Ce contents normally both Ce^{3+} and Ce^{4+} (non-fluorescing) ions are. The absorption spectra of glasses containing both Ce^{3+}/Ce^{4+} ions have characteristic bands within a 200–400-nm range (not measurable using our spectral equipment); so their transformations under β-irradiation ($Ce^{3+} \leftrightarrow Ce^{4+}$) don't have matter for the spectral changes we detected in VIS. In the meantime, the ones of $Ce^{3+}h^{+}$ and $Ce^{4+}e^{-}$ defect centers are expectedly located in VIS (see above), on one hand, and, on the other hand, the detected spectral changes at β-irradiation also occur in VIS (band 2). Therefore, formation of (metastable) centers $Ce^{3+}h^{+}/Ce^{4+}e^{-}$ as the result is a worthy proposal.

Furthermore, we suppose that one more process, VIS fluorescence stimulated by β-irradiation via 5d→4f transition (Ce^{3+}) and spectrally centered at ~350–550 nm [19,23,33,34,44–48,51,54,62] should enter in action because of matching by this fluorescence the IA spectral bands 1 and 2 (see Figs. 3 and 4). Noteworthy, ~350–550-nm "radio-fluorescence" frequently serves a measure for sensing dose of ionizing radiations using Ce doped materials [19,22,34,45,51,52,62,63].

The IA bands 1 (~3.0 eV) and 2 (~2.4 eV) have been doubtlessly separated above (see Fig. 4). The first of them, in Ce-doped and Ce/Au-codoped fibers, has seemingly the same origin as the one in the Ce free fiber (see Fig. 2), i.e. it most probably belongs to one, most simply organized, type of the two NBOHC's centers, inherent to silica. The other stems as we think from Ce doping of the fibers: It is seen from Fig. 2 that such band doesn't exist in the reference Ce free fiber. In the meantime, the irradiated Ce free fiber demonstrates ~600-nm band, not surely but quite probably attributing the other type of NBOHC's [39], apparently absent in both irradiated Ce-doped fibers; compare spectra 1 to 3 shown in Fig. 2. The fact that the dose dependences of IA shown in main frames of Fig. 4 have different characters for the fibers points on different origins of the centers represented by absorption bands 1 and 2. Therefore, our hypothesis that ~3.0-eV band stems from NBOHC's whereas the ~2.4-eV one is associated with a Ce-related center ($Ce^{3+}h^{+}/Ce^{3+}e^{-}$) seems to be relevant. Furthermore, Si-

#198435 - $15.00 USD Received 30 Sep 2013; revised 2 Dec 2013; accepted 3 Dec 2013; published 7 Feb 2014

and Al-related centers, characterized by intensive extinction in the UV and VIS spectral regions, can be also formed by ionizing radiations. In our case (alumino-silicate core glass of Ce-doped and Ce/Au-codoped fibers), such "point" defects as Al-E' and Al-oxygen-deficient centers can be as well created at trapping secondary electrons and holes born at β-irradiation (phosphorous presented in small content in the fibers seemingly plays a little effect).

Thus, the processes roughly schematized as $Ce^{3+} \leftrightarrow Ce^{4+}$ seem to be nearly a sole way to address the spectral transformations shown in Figs. 2–4, viz., via the formation in Ce- and Ce/Au-doped fibers of metastable states $Ce^{3+}h^{+}/Ce^{4+}e^{-}$.

It deserves mentioning that overall sensitivity to β-irradiation (overall IA loss) of Ce-doped fiber is higher than of Ce/Au-codoped one. This may signify that the core glass containing gold is more stable than glass only containing Ce, regarding the above discussed processes. On the other hand, deviations in the experimental data demonstrating kinetics of IA *vs*. β-irradiation dose for Ce-doped and Ce/Au-codoped fibers (refer to IA spectra in Fig. 3 and to dose dependences in Fig. 4) are more pronounced in the former than in the latter fiber, with a possible explanation being that co-doping with Au gives rise to the core-glass system more ordered. This property seems to have impact for establishing almost the same path kinetics of defect centers formation and for lesser impact of other factors in this type of fiber.

As we noted in introduction, Au co-doping of Ce-doped fiber was expected to improve its radiation resistance. From one side, it is known that due to high temperature-induced self-reduction reactions during the MCVD processes, Au ions are easily transformed into Au^0 atoms and clustered into nanoparticles in silica glass. However, considering Ce ions as an effective trap centers (by providing and capturing charge carriers in host materials [64]), their presence prevents formation of Au nanoparticles and leads to oxidizing (to AuO_x) at the stage of making of a fiber preform [65]. Aluminum also plays an important role through suppressing formation of Au nanoparticles [65]. From the other side, the electron density on non-bridging oxygen in silica matrix will be polarized in the presence of positively charged Au ions, which reduces the probability of coordination with Ce ions. As a result, Ce ions' segregation is disturbed in the presence of Au. Notice that in silica glass Ce acts normally as a network modifier but, when glass is co-doped with Au, it also serves as a segregation inhibitor. Thus, supposedly Ce/Au codoping would ultimately result in homogenization of glass and therefore to its resistance to different kinds of irradiation, including the performed β-irradiation.

Resuming, Ce/Au co-doped fibers appear to be a better choice for dosimetry and other applications.

4.3. Optically bleached fibers

Let's now briefly discuss the effect of partial bleaching of β-irradiated Ce-doped and Ce/Au-codoped fibers under the action of low-power VIS (543 nm: He-Ne laser) and UV (lamp) light; see Figs. 5–7. Whereas doubtless explanation is hard of what its nature is a discourse about the matters involved can be made. The processes responsible for recombination of radiation-induced defects or color centers, seen as IA fading (bleaching) of darkened fibers, can be thermally- and/or optically-induced. Bleaching, with its result being decreasing IA *vs.* time, seems to be an example of mainly optically-induced recombination of both types of centers, NBOHC's and Ce-related $Ce^{3+}h^{+}$ (assumed to be represented by bands 1 and 2, respectively). However, the thermal mechanism cannot be presumably excluded in the circumstance of exposing the irradiated fibers to optical bleaching. Indeed, at high IA established after irradiation and non-vanishing optical power launched into the darkened fibers, weak but non-vanishing heating of the samples should arise.

As seen from Fig. 5(d) and Fig. 7 (c) IA decreases almost exponentially at the beginning of bleaching. However, within the whole interval of optical bleaching, IA in bands 1 and 2 is seen to fade (in terms of negative AD at exposing the fibers to 543-nm laser, see Figs. 5 (a) and 5(b), and in terms of shift to shorter wavelength of the transmission edge measured at a 3-dB level at exposure to UV light, see Figs. 7 (a) and 7(c), obeying a kind of the "stretched exponent" law [39,56–58]. An explanation for this, strongly non-exponential, behavior can be

#198435 - $15.00 USD Received 30 Sep 2013; revised 2 Dec 2013; accepted 3 Dec 2013; published 7 Feb 2014

not only complexity of the mechanisms involved at optical bleaching but also a trivial fact of limited "penetration" length of bleaching light into a fiber sample (especially in the case of 543-nm bleaching), which in turn depends on a current stage of bleaching.

Concerning the essence of the processes involved at IA optical bleaching, we can, at the current stage of our knowledge, only tentatively propose them. If our attribution of IA bands 1 and 2 as stemming from NBOHC's and Ce-related $Ce^{3+}h^{+}$ centers is correct, then these centers, formed at trapping free holes, should be progressively breaking via the holes' de-trapping and annihilating with free electrons born at interaction of 543-nm or UV light. Weak intensity of bleaching light is guessed to result in producing of mainly extra electrons than holes in the core glass matrix, which would cause dominance of the processes within the hole-trapped centers, such as NBOHC (~3.0 eV band) and $Ce^{3+}h^{+}$ ones (~2.4 eV band). Note that a strong candidate to be responsible for the production of e^{-} at the UV/VIS excitation may be Ce^{3+} ions themselves [17,40]. Thus, regarding for instance Ce-related $Ce^{3+}h^{+}$ center, a reaction $Ce^{3+}h^{+} + e^{-} \rightarrow Ce^{3+}$ can go at optical bleaching.

Comparison of the bleaching effect in Ce-doped (without Au co-doping) and Ce/Au-codoped fibers show that it is less expressed in the latter than in the former, which is most probably related to lower susceptibility to exterior influence of Ce/Au-codoped fiber (a consequence of its more ordered glass network, already remarked). However, more experimental materials are required for confirming or rejecting the hypothesis.

5. Conclusions

The technique to fabricate Ce doped large-core fibers with alumino-phospho-silicate core glass is reported as well as their basic absorptive properties in as-drawn (pristine) state, after irradiation with a beam of high-energy electrons, and, finally, after posterior optical bleaching by VIS/UV low-power light. The fibers were made in two implementations, in one being doped solely with Ce and in the other with Ce and Au, with an idea of comparison of advantages and disadvantages of these two for sensing ionizing radiations (dosimetry) and future work with silica fibers co-doped with Yb, Er, or Ho and Ce for lasing / amplifying in the conditions of harmful (nuclear plants, space, etc.) environments.

Notice that co-doping of Ce-doped silica fiber (or glass) with Au has been made for the first time to the best of our knowledge (the presence of Au in the samples [66] was established non-intentionally and was not discussed in details). The reported experiments along with the discussions permit us to conclude that such fibers are quite useful for practice. A few news of the present study, regarding the experimental details of the fibers' absorption spectra transformations at high-energy electron irradiation and posterior optical bleaching along with the role of reactions $Ce^{3+} \leftrightarrow Ce^{4+}$ as occurring via metastable $Ce^{3+}h^{+}/Ce^{4+}e^{-}$, still hypothetical but congruent to the experiments (and not contradicting the literature data), deserves emphasizing.

We didn't discuss a possible role of the spectral changes in refractive index of Ce doped fibers at β-irradiation and optical bleaching, which ought to happen in virtue of strong induced absorption and according to the Kramers–Kroënig relations. In future, a study of the refractive-index nonlinearity is planned using analogous Ce-doped and Ce/Au-codoped fibers with smaller core area.

Acknowledgments

This work was supported in part by the CONACyT (Project 167945), Mexico.

#198435 - $15.00 USD Received 30 Sep 2013; revised 2 Dec 2013; accepted 3 Dec 2013; published 7 Feb 2014